

## Fracture Criterion of Elastic-Plastic Crack under Mixed Mode Condition Based on CED (Crack Energy Density)

Takao UTSUNOMIYA

*Niihama National College of Technology, Niihama, Japan*

Katsuhiko WATANABE

*University of Tokyo, Tokyo, Japan*

### ABSTRACT

The CED (Crack Energy Density) in an arbitrary direction,  $\mathcal{E}_\varphi$ , is defined as the quantity which has the meaning of strain energy area density in the plane containing a crack front line without any restriction on constitutive equation. We may expect that, as far as the opening type fracture occurs, a mixed mode crack begins to grow in the direction  $\varphi$  where  $\mathcal{E}_\varphi^I$  (mode I contribution of  $\mathcal{E}_\varphi$ ) takes the maximum value,  $\mathcal{E}_{\varphi_{max}}^I$ , when  $\mathcal{E}_{\varphi_{max}}^I$  reaches a critical value peculiar to a material (we call this criterion  $\mathcal{E}_{\varphi_{max}}^I$  criterion). In this paper, the applicability of this  $\mathcal{E}_{\varphi_{max}}^I$  criterion to elastic-plastic fractures is studied based on the fracture experiments on specimens of Aluminum alloy with a crack inclined to the loading axis and it is demonstrated that the onset and the direction of crack growth can be estimated by  $\mathcal{E}_{\varphi_{max}}^I$  criterion in either case of fractures with relatively small yielding region and those with large yielding region. The applicability of  $\mathcal{E}_{\varphi_{max}}^I$  criterion to elastic (quasi-elastic) fractures is also shown through the comparison of the results by  $\mathcal{E}_{\varphi_{max}}^I$  criterion with the results by other criteria and experimental results.

### 1 INTRODUCTION

Not a few cracks in actual structures are under mixed mode condition. So, in order to evaluate their strengths, it is necessary to establish the fracture criterion of a crack under mixed mode condition. As to the mixed mode criteria,  $\sigma_{\theta_{max}}$  criterion (Erdogan and Sih 1963),  $S_{min}$  criterion (Sih 1973),  $\mathcal{G}_{max}$  criterion (Kageyama and Okamura 1982) etc. have been proposed for elastic (quasi-elastic) fractures, and it is known that the difference between the results by these criteria is not so large and they can almost explain experimental results. On the other hand, some fracture criteria have been proposed based on  $J$ -integral for elastic-plastic fractures (Takamatsu and Ichikawa 1987, Sakata et al. 1985, Cotterell et al. 1982 etc.). However, these criteria are not natural extensions of the criteria for elastic (quasi-elastic) fractures above and their physical meanings are not so clear. Moreover, these criteria cannot be applied when the ratio of mode II deformation becomes large and they cannot predict the direction of crack growth. Accordingly, it is considered that the mixed mode fracture criterion, especially for elastic-plastic fractures, has yet to be established.

The CED (Crack Energy Density) was proposed by one of authors as a parameter which can be defined without any restriction on constitutive equation and has the meaning of strain energy area density throughout the life of a crack consistently (Watanabe 1981, 1983). In order to apply this concept to a crack which does not grow in the self-similar direction, the authors showed that the CED can be defined also in any direction at a

crack tip besides in the self-similar direction (Watanabe and Shiomi 1985) and the CED in an arbitrary direction,  $\mathcal{E}_\varphi$ , can be divided into the contributions of each mode in general ( $\mathcal{E}_\varphi = \mathcal{E}_\varphi^I + \mathcal{E}_\varphi^{II} + \mathcal{E}_\varphi^{III}$ ;  $\mathcal{E}_\varphi^I, \mathcal{E}_\varphi^{II}$  and  $\mathcal{E}_\varphi^{III}$  are the contributions of mode *I*, *II* and *III* respectively) (Watanabe and Utsunomiya 1987). These quantities can be evaluated by stress intensity factors especially in case of elastic problem (Watanabe and Shiomi 1985) and, in either case of elastic and elastic-plastic problems, they can be evaluated by path-independent integrals (Watanabe and Utsunomiya 1987).  $\mathcal{E}_\varphi$  can be evaluated also by the relationship between  $\mathcal{E}_\varphi$  and load-displacement curves (Watanabe et al. 1989).

Based on this series of researches, the authors proposed recently the criterion that, as far as the opening type fracture occurs, a crack under mixed mode condition begins to grow in the direction  $\varphi$  where  $\mathcal{E}_\varphi^I$  takes the maximum value,  $\mathcal{E}_{\varphi max}^I$ , when  $\mathcal{E}_{\varphi max}^I$  reaches a critical value peculiar to a material (we call this criterion  $\mathcal{E}_{\varphi max}^I$  criterion) (Watanabe and Utsunomiya 1990). In this paper, the applicability of  $\mathcal{E}_{\varphi max}^I$  criterion not only to elastic fractures but also to elastic-plastic fractures under mixed mode condition is studied. As for elastic (quasi-elastic) fracture,  $\mathcal{E}_{\varphi max}^I$  criterion is compared with other criteria and, moreover, it is applied to the experimental results of quasi-elastic fractures of specimens with an inclined crack under tensile loading. As for elastic-plastic fractures, at first,  $\mathcal{E}_{\varphi max}^I$  criterion is applied to the experiment of a thin sheet specimen with an inclined crack under tensile loading by Takamatsu et al. (Takamatsu and Ichikawa 1987) in which the fracture occurs with relatively small yielding region. In the second, the similar fracture experiment of a specimen with an inclined crack under tensile loading is carried out and  $\mathcal{E}_{\varphi max}^I$  criterion is applied to the experimental result. In this experiment, the fracture occurs with large scale yielding region. Through these results, it is shown that  $\mathcal{E}_{\varphi max}^I$  criterion is effective from completely elastic fracture to elastic-plastic fracture with large yielding region in a unified way.

## 2 DEFINITION OF CED IN AN ARBITRARY DIRECTION AND MIXED MODE FRACTURE CRITERION

In this chapter, the definition of the CED in an arbitrary direction,  $\mathcal{E}_\varphi$ , which is used as the fracture parameter in this paper and its evaluation methods are shown briefly. Moreover,  $\mathcal{E}_{\varphi max}^I$  criterion is explained.

### 2.1 Definition of CED in an arbitrary direction

Think of a crack ( $\rho=0$ ) as the limit when the tip radius,  $\rho$ , of each notch shown in Fig.1(a) and (b) approaches zero. We call tip shapes of Fig.1(a) and (b) a circular notch and a semicircular notch respectively. Although a circular notch may look strange, it is useful in the evaluation of  $\mathcal{E}_\varphi$  etc. through finite element analyses (Watanabe and Utsunomiya 1987). Consider a two-dimensional continuum with one of these two notches in which applied forces in the  $X_1 - X_2$  plane cause plane strain or plane stress state and those in the  $X_3$  direction do antiplane deformation.  $(X_1, X_2, X_3)$  is a fixed coordinate system and  $(x_1, x_2, x_3)$  is a moving coordinate system which is defined by rotating  $(X_1, X_2, X_3)$  by an amount  $\varphi$  around the  $X_3$  axis. The CED in the semi-infinite plane containing  $x_1 (> 0)$  and  $x_3$  axes (this plane is called  $\varphi$  plane hereafter) (Watanabe and Shiomi 1985) is defined as

$$\mathcal{E}_\varphi = \lim_{\rho \rightarrow 0} \mathcal{E}_\varphi(\rho) \quad (1)$$

where

$$\mathcal{E}_\varphi(\rho) = \int_{\Gamma_0^+} W dx_2$$

Here,  $W$  is the strain energy density given by

$$\mathcal{E}_\varphi(\rho) = \int_0^t \sigma_{ij} d\epsilon_{ij} \quad (i, j = 1, 2, 3) \quad (2)$$

where  $t$  is the present time,  $\sigma_{ij}$  and  $\epsilon_{ij}$  are the components of stress and strain tensors defined in  $(x_1, x_2, x_3)$  coordinate system respectively, and the integration is carried out along an actual loading path from the time zero to the present time  $t$ .  $\Gamma_0^+$  is the part of the path  $\Gamma_0^+ - \Gamma_0^-$  along the notch tip (cf. Fig.1), and it is contained in the  $\varphi$  plane in the limit when  $\rho \rightarrow 0$  [ $\Gamma_0^-$  corresponds to the part contained in the  $(\varphi - 180^\circ)$  plane in the limit when  $\rho \rightarrow 0$ ].

This  $\mathcal{E}_\varphi$  means 'the energy, per unit area about  $\varphi$  plane, absorbed at a crack tip' and is independent of the shape of notch in the limit when  $\rho \rightarrow 0$  (Watanabe and Utsunomiya 1987). It was shown previously that  $\sigma_{ij}$  and  $d\epsilon_{ij}$  in Eq.(2) can be divided, in general, into three parts which cause mode *I*, mode *II* and mode *III* deformations respectively and  $\mathcal{E}_\varphi$  can be divided into the contributions of each deformation mode without any restriction on constitutive equation (that is,  $\mathcal{E}_\varphi = \mathcal{E}_\varphi^I + \mathcal{E}_\varphi^{II} + \mathcal{E}_\varphi^{III}$ ,  $\mathcal{E}_\varphi^I$ ; mode *I* contribution,  $\mathcal{E}_\varphi^{II}$ ; mode *II* contribution,  $\mathcal{E}_\varphi^{III}$ ; mode *III* contribution)(Watanabe and Utsunomiya 1987).

$\mathcal{E}_\varphi$  and the contributions of each mode can be evaluated as follows;

(1) For an elastic problem, we can evaluate  $\mathcal{E}_\varphi$ ,  $\mathcal{E}_\varphi^I$  etc. through the stress intensity factors when they are known (Watanabe and Shiomi 1985).

The following two methods can be applied in either case of elastic and elastic-plastic problems.

(2)  $\mathcal{E}_\varphi$ ,  $\mathcal{E}_\varphi^I$  etc. can be expressed by path-independent integrals (domain integrals) defined by using an arbitrary path  $\Gamma + \Gamma_u$  surrounding path  $\Gamma_0^+$  and the area  $A$  surrounded by a closed path  $\Gamma + \Gamma_u - \Gamma_0^+$  shown in Fig.1(a) and (b). They can be evaluated by these integrals through finite element analyses with no restriction on constitutive equation (Watanabe and Utsunomiya 1987, 1990).

(3) By considering the difference of the strain energies for two specimens which have a straight notch and a kinked notch, we can derive the relationship between  $\mathcal{E}_\varphi$  and load-displacement curves. Based on the relationship,  $\mathcal{E}_\varphi$  can be evaluated by load-loading point displacement curves obtained from each specimen under tensile loading (Watanabe et al. 1989).

In this paper,  $\mathcal{E}_\varphi$  and the contributions of each mode are evaluated by using these three methods.

## 2.2 $\mathcal{E}_{\varphi max}^I$ criterion

In case of mode *I* crack,  $\mathcal{E}_\varphi^I$  takes the maximum value in the direction of  $\varphi=0^\circ$  (in the self-similar direction) and its value is almost equal to that of  $J_I$  (strictly equal under deformation theory) (Watanabe and Utsunomiya 1989). Therefore, the relation as  $J_I \doteq \mathcal{E}_{\varphi max}^I = \mathcal{E}_{\varphi=0^\circ}^I = (\mathcal{E}^I)_i \doteq (J_I)_i$  [ $\mathcal{E}_{\varphi max}^I$  is the maximum value of  $\mathcal{E}_\varphi^I$ , and  $(\mathcal{E}^I)_i$  and  $(J_I)_i$  are the values of  $\mathcal{E}_{\varphi=0^\circ}^I$  and  $(J_I)_i$ , respectively, when a crack starts to grow] holds and  $J$  criterion which has been widely accepted as the fracture criterion of a mode *I* crack can be regarded as the criterion that a crack starts to grow in the direction of  $\varphi=0^\circ$  where  $\mathcal{E}_\varphi^I$  takes the maximum value  $\mathcal{E}_{\varphi max}^I$  when  $\mathcal{E}_{\varphi max}^I$  reaches the critical value. As a natural extension of this fact to the fracture of a mixed mode crack,  $\mathcal{E}_{\varphi max}^I$  criterion is given as follows; 'As far as the opening type fracture occurs, a crack begins to grow in the direction where  $\mathcal{E}_\varphi^I$

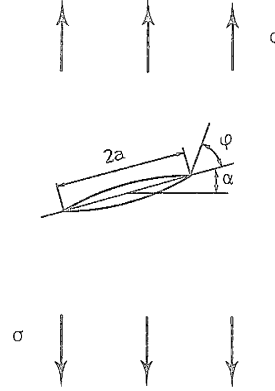
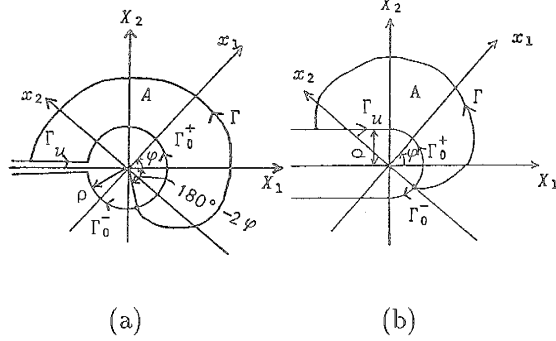


Fig.1 Circular notch and semicircular notch      Fig.2 Inclined crack in an infinite plate

takes  $\mathcal{E}_{\varphi_{max}}^I$  when  $\mathcal{E}_{\varphi_{max}}^I$  reaches the critical value peculiar to a material' (Watanabe and Utsunomiya 1990).

In this paper, the applicability of this  $\mathcal{E}_{\varphi_{max}}^I$  criterion to the fracture of a two-dimensional inclined crack under tensile loading is discussed. For an elastic fracture, the value of  $\mathcal{E}_{\varphi_{max}}^I$  and  $\varphi$  where  $\mathcal{E}_{\varphi}^I$  takes  $\mathcal{E}_{\varphi_{max}}^I$  are determined based on the results evaluated by the theoretical relation between  $\mathcal{E}_{\varphi}^I$  and stress intensity factors. For an elastic-plastic fracture, finite element analyses are carried out,  $\mathcal{E}_{\varphi}$  and  $\mathcal{E}_{\varphi}^I$  are evaluated by path-independent integrals and, moreover,  $\mathcal{E}_{\varphi}$  is evaluated by the method based on load-displacement curves. Then, through these results,  $\mathcal{E}_{\varphi_{max}}^I$  and  $\varphi$  where  $\mathcal{E}_{\varphi}^I$  takes  $\mathcal{E}_{\varphi_{max}}^I$  are determined as follows (Watanabe and Utsunomiya 1990);

- (1) Obtain  $\varphi$  for  $\mathcal{E}_{\varphi_{max}}^I$  from the results by path-independent integral.
- (2) Evaluate  $\mathcal{E}_{\varphi}$  in the direction above by the method based on load-displacement curves and regard it as  $\mathcal{E}_{\varphi_{max}}^I$ .

### 3 APPLICABILITY OF $\mathcal{E}_{\varphi_{max}}^I$ CRITERION TO ELASTIC (QUASI-ELASTIC) FRACTURE

In this chapter, the  $\mathcal{E}_{\varphi_{max}}^I$  criterion is applied to the mixed mode elastic (quasi-elastic) fracture of a two-dimensional inclined crack under uniform tensile stress and, through the comparisons with the results based on other criteria and experimental results, the applicability of  $\mathcal{E}_{\varphi_{max}}^I$  criterion to mixed-mode elastic (quasi-elastic) fractures is discussed.

#### 3.1 Comparisons with other criteria

$\mathcal{E}_{\varphi_{max}}^I$  criterion and other criteria ( $\sigma_{\theta_{max}}$  criterion,  $S_{min}$  criterion and  $\mathcal{G}_{max}$  criterion) are applied to an inclined crack in an infinite plate under uniform tensile stress here (cf. Fig.2) and the proportions of  $K_I$  and  $K_{II}$  at fracture and the directions of crack growth by each criterion are compared.

Mode I and mode II stress intensity factors for a crack shown in Fig.2 are given by

$$\begin{aligned} K_I &= \sigma \sqrt{\pi a} \sin^2(90^\circ - \alpha) \\ K_{II} &= \sigma \sqrt{\pi a} \sin(90^\circ - \alpha) \cos(90^\circ - \alpha) \end{aligned} \quad (3)$$

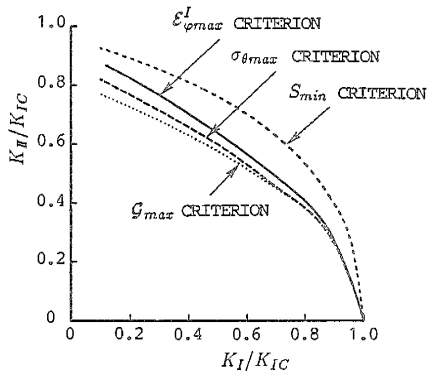


Fig.3 Proportion of  $K_I$  and  $K_{II}$  at fracture (Comparison with other criteria)

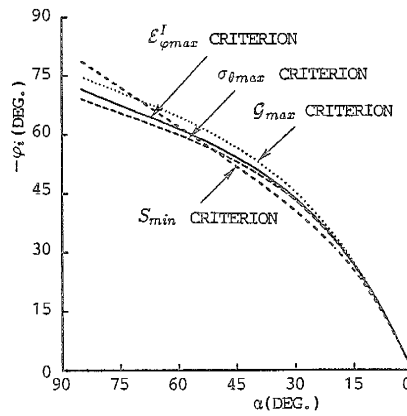


Fig.4 Crack growth direction (Comparison with other criteria)

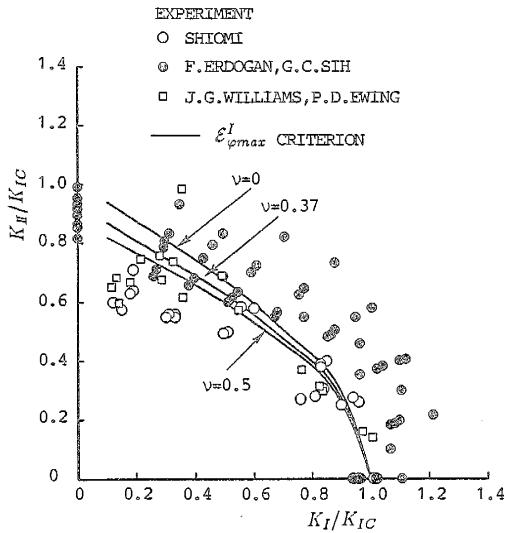


Fig.5 Proportion of  $K_I$  and  $K_{II}$  at fracture (Comparison with experimental results of quasi-elastic fracture)

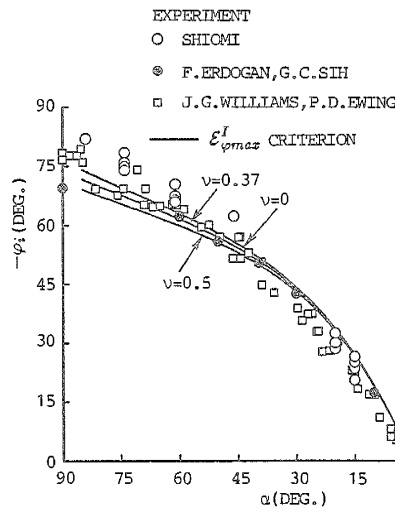


Fig.6 Crack growth direction (Comparison with experimental results of quasi-elastic fracture)

Each parameter is evaluated through these stress intensity factors. Poisson's ratio  $\nu$  is 0.3. Figs.3 and 4 show the proportion of  $K_I$  and  $K_{II}$  at fracture and the relationship between the inclination angle of crack and the direction of crack growth,  $\varphi_i$ , determined by each criterion, respectively. In these figures, the tendencies of the curves by  $E^I_{\varphi_{max}}$  criterion are a little different from those by  $S_{min}$  criterion, but are almost the same as those by  $\sigma_{\theta_{max}}$  and  $G_{max}$  criteria.

### 3.2 Comparisons with elastic (quasi-elastic) fracture experiments

Quasi-elastic fracture experiments of two-dimensional specimens with an inclined crack under tensile loading were carried out by Shiomi (Shiomi 1981), Erdogan-Sih (Erdogan and Sih 1963), Williams-Ewing (Williams and Ewing 1972) etc.. The materials used in the

experiments are epoxy resin (Young's modulus  $E=3.03\text{GPa}$  and Poisson's ratio  $\nu=0.37$ ; Shiomi), plexiglass (Erdogan-Sih) and PMMA (Williams-Ewing) respectively. They obtained the proportions of  $K_I$  and  $K_{II}$  at fracture and the direction where a crack starts to grow. In Figs.5 and 6, those experimental results are compared with the results by  $\mathcal{E}_{\varphi_{max}}^I$  criterion for plane strain state. In the figures, the curves when  $\nu=0$  and  $\nu=0.5$  are shown in addition to that of  $\nu=0.37$  ( $\nu=0.37$  in the experiment by Shiomi but Poisson's ratios for the experiments of Erdogan-Sih and Williams-Ewing are not given).  $\mathcal{E}_{\varphi_{max}}^I$  is evaluated through the solutions of stress intensity factors (Kitagawa and Yuuki 1977).

### 3.3 Applicability of $\mathcal{E}_{\varphi_{max}}^I$ criterion

Fig.3 ~ Fig.6 show that the result by  $\mathcal{E}_{\varphi_{max}}^I$  criterion almost coincides with the results by  $\sigma_{\theta_{max}}$  criterion and  $\mathcal{G}_{max}$  criterion which have been most accepted as the fracture criterion of a quasi-elastic crack and its tendency agrees, on the whole, with those experimental results. Thus, it can be concluded at least that  $\mathcal{E}_{\varphi_{max}}^I$  criterion is effective in the same degree as those of  $\sigma_{\theta_{max}}$  criterion and  $\mathcal{G}_{max}$  criterion.

## 4 APPLICABILITY OF $\mathcal{E}_{\varphi_{max}}^I$ CRITERION TO ELASTIC-PLASTIC FRACTURE WITH RELATIVELY SMALL YIELDING REGION

We carried out elastic-plastic finite element analyses simulating the fracture experiment of a thin sheet specimen with a crack inclined to the loading axis by Takamatsu et al. and studied the applicability of  $\mathcal{E}_{\varphi_{max}}^I$  criterion (Watanabe and Utsunomiya 1990). In these analyses, Aluminum alloy 2024-T3 is supposed corresponding to the experiment. Fig.7 shows the configuration of the specimen used in the experiment by Takamatsu et al. and Fig.8 shows an example of yielding region when a crack starts to grow by finite element analysis. From Fig.8, it is found that the yielding region in the experiment by Takamatsu et al. is not so large when a crack starts to grow.  $(J_I)_i$  [ $\frac{1}{2}(\mathcal{E}^I)_i$ ] from the experiment by Takamatsu et al. is  $0.0164\text{J}/\text{mm}^2$ . Fig.9 shows the relationship between  $(\sigma_{net})_i$  and  $\alpha$  when  $\mathcal{E}_{\varphi_{max}}^I$  criterion is applied to the experiment by Takamatsu et al.  $(\sigma_{net})_i$  is the mean stress in the minimum cross-section perpendicular to the loading axis [ $(\sigma_{net})_i = P/(2W - 2a \cos \alpha)B$ , where  $B$  is the thickness of the specimen and  $P$  is the tensile load]. In the figure, the results by  $J_I + J_{II} = (J_I)_i$  criterion ( $J_I$  and  $J_{II}$  are mode I and mode II contributions of  $J$ -integral) by Sakata et al. and the result by  $J_I + cJ_{II} = (J_I)_i$  criterion are also shown [ $c = (J_I)_i/(J_{II})_i = 1.56$ ,  $(J_{II})_i = 0.0105\text{J}/\text{mm}^2$ ]. Moreover, in order to examine the applicability of the criteria for elastic (quasi-elastic) fracture to this experimental result, the results by  $\sigma_{\theta_{max}}$  criterion and  $\mathcal{E}_{\varphi_{max}}^I$  criterion are also shown by using the stress intensity factors  $(K_I)_\alpha$  and  $(K_{II})_\alpha$  evaluated by

$$\begin{aligned} (J_I)_i &= \frac{(K_I)_\alpha^2 + (K_{II})_\alpha^2}{E} \\ (K_I)_\alpha &= \sigma \sqrt{\pi a} \cdot F_I \\ (K_{II})_\alpha &= \sigma \sqrt{\pi a} \cdot F_{II} \quad , \quad \sigma = P/(2WB) \end{aligned} \quad (4)$$

Here,  $\mathcal{E}_{\varphi_{max}}^I$  is evaluated through the theoretical relation between  $\mathcal{E}_\varphi^I$  and stress intensity factors. For reference, the line of  $\sigma_{ys}$  is shown in Fig.9. From this figure, it is found that, when elastic-plastic deformations considered, the result by  $\mathcal{E}_{\varphi_{max}}^I$  criterion agrees well with the experimental result over the entire range of  $\alpha$ . Especially, although the results by other criteria become larger than the experimental result when  $\alpha$  becomes large

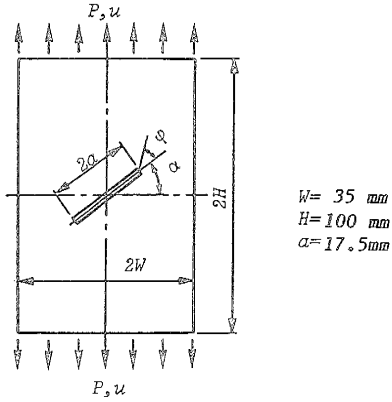


Fig.7 Specimen configuration

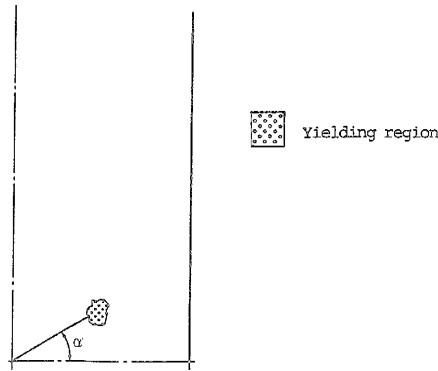


Fig.8 Yielding region of specimen  
( $\alpha = 30^\circ$ )

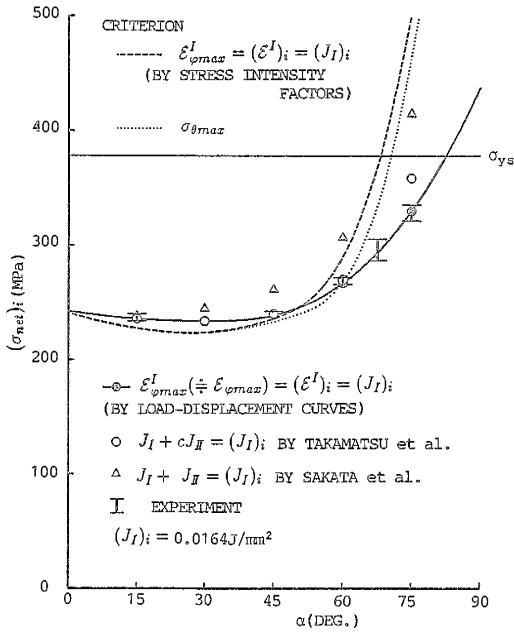


Fig.9 Relationship between  $(\sigma_{net})_i$  and  $\alpha$

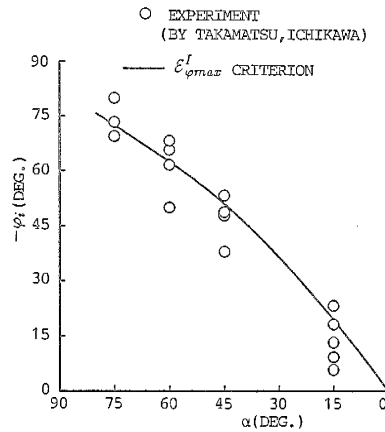


Fig.10 Comparison between crack growth direction by experiment and  $\mathcal{E}_{\varphi_{max}}^I$  criterion

(the mode II deformation becomes large), the result by  $\mathcal{E}_{\varphi_{max}}^I$  criterion agrees well with the experimental result. As a crack starts to grow with relatively small yielding region,  $(\sigma_{net})_i$  by the experiment is smaller than  $\sigma_{ys}$  and, when  $\alpha$  is small, the criteria for elastic (quasi-elastic) fracture ( $\sigma_{\theta_{max}}$  criterion and  $\mathcal{E}_{\varphi_{max}}^I$  criterion evaluated through stress intensity factors) can be applied. In Fig.10, the direction where  $\mathcal{E}_{\varphi}^I = \mathcal{E}_{\varphi_{max}}^I$  is compared with the experimental result by Takamatsu et al.. From the figure, it is found that the direction where a crack starts to grow can be also estimated by  $\mathcal{E}_{\varphi_{max}}^I$  criterion in case of elastic-

plastic fracture with relatively small yielding region. Accordingly, it is concluded that  $\mathcal{E}_{\varphi_{max}}^I$  criterion can be applied to elastic-plastic fracture with relatively small yielding region.

## 5 APPLICABILITY OF $\mathcal{E}_{\varphi_{max}}^I$ CRITERION TO ELASTIC-PLASTIC FRACTURE WITH LARGE YIELDING REGION

In this chapter, the fracture experiment of the specimen with an inclined crack under tensile loading similar to the experiment by Takamatsu et al. is carried out and  $\mathcal{E}_{\varphi_{max}}^I$  criterion is applied to this experimental result. In the experiment, the fracture occurs with large yielding region. Through the applicability to this experiment and the results mentioned in chapters 3 and 4, it is shown that  $\mathcal{E}_{\varphi_{max}}^I$  criterion is hopeful as the criterion that can be applied to all kinds of elastic or elastic-plastic fractures.

### 5.1 Mixed-mode fracture experiment

The material used in the experiment is Aluminum alloy 2024-T3 and the configuration of the specimen is shown in Fig.11. Thickness of the specimen is 2mm. The specimens are made up as follows. A specimen with a chevron-type center-crack for introducing a pre-fatigue crack, in which the cracked plane is perpendicular to the direction of cyclic load, is prepared first and a pre-fatigue crack is finished. Then, the specimen with an inclined crack required is cut out so that the loading axis in fracture experiment coincides with the rolling direction. As to the inclination angle of a crack,  $\alpha$ , four cases ( $\alpha = 0^\circ, 30^\circ, 60^\circ, 75^\circ$ ) are taken and the initial crack length is  $a/W = 0.4$ . To form a crack, a chevron-type crack is made up first by 12mm ( $a/W = 0.3$ ) and a pre-fatigue crack is introduced by 16mm ( $a/W = 0.4$ ). The loading point displacement, which is defined as the relative displacement between the upper and lower sections that are 40mm away from a center-crack as shown by chain lines in Fig.11, is measured by a displacement gauge (0 ~ +20mm in full scale). The fracture experiment is carried out using an Instron type testing machine (98MN in load capacity) and the relative velocity between the crosshead and the screw rod is 0.25 mm/min. The region around crack tip is observed by a microscope and the onset of crack growth is determined. Simultaneously, the situations in the neighborhood of a crack is recorded by photographs and the direction of crack growth is determined from these photographs.

In order to obtain the material property of Aluminum alloy, the L-T specimen for material test of which the tensile direction is perpendicular to the rolling direction and the R-D specimen of which the tensile direction is parallel to the rolling direction are prepared and the material tests for them are carried out. The relative velocities of the crosshead are 0.25mm/min and 1.0mm/min. Fig.12 shows the relation between stress and strain. From Fig.12, it can be almost said that this Aluminum alloy is not anisotropic and the material property does not depend on the relative velocity of the crosshead. As for the obtained material constants, Young's modulus  $E = 69.78$  GPa, Poisson's ratio  $\nu = 0.326$ , Yield stress  $\sigma_{ys} = 378.3$  MPa and  $C = 648.0$  MPa,  $n = 0.117$  and  $a = 0.01$  in  $\bar{\sigma} = C(a + \bar{\epsilon}_p)^n$ .

### 5.2 Finite element analyses

Elastic-plastic finite element analysis corresponding to the experiment is carried until a crack starts to grow.  $\mathcal{E}_\varphi$  and  $\mathcal{E}_{\varphi_{max}}^I$  are evaluated by path-independent integrals and  $\mathcal{E}_\varphi$  is evaluated also by the method based on load-displacement curves.  $\mathcal{E}_{\varphi_{max}}^I$  and  $\varphi$  where  $\mathcal{E}_\varphi^I$  takes  $\mathcal{E}_{\varphi_{max}}^I$  are evaluated based on the method mentioned in section 2.2 with sufficient accuracy. The analyses are carried out for the half region of the specimen because of the skew-symmetric property. Triangle constant strain elements are employed and plane stress state is supposed. In the evaluation by path-independent integrals, a circular notch ( $\rho/W = 0.00114$ ) is employed and the total number of elements and nodal points are 1898



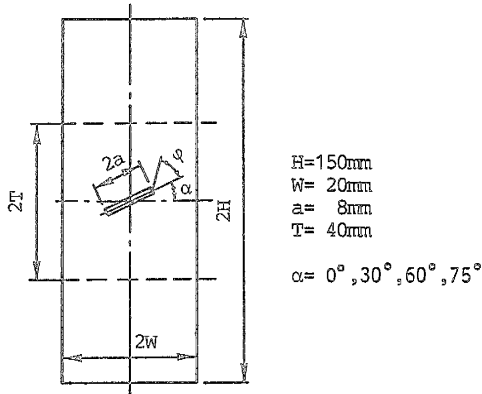


Fig.11 Specimen configuration

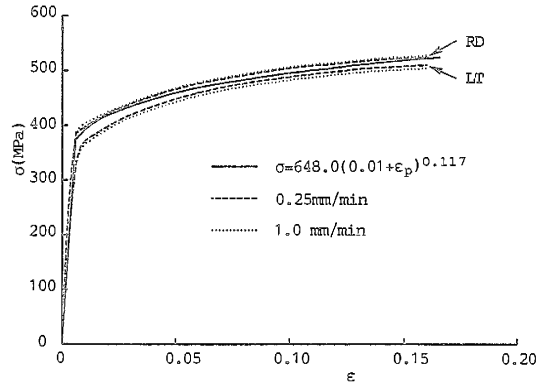


Fig.12 Stress-strain curve

and 1034 respectively. In case of the method based on load-displacement curves, a crack ( $\rho = 0$ ) is employed and the total number of elements and nodal points are 1630 and 868 respectively.

### 5.3 Applicability of $\mathcal{E}_{\varphi_{max}}^I$ criterion

Fig.13 is an example of yielding region when a crack starts to grow obtained by this analysis, and it shows that the yielding region goes across the ligament and, in the experiment, the fracture occurs with considerably large yielding region. Table 1 shows the loading point displacement and the value of  $\mathcal{E}_{\varphi_{max}}^I$  for each  $\alpha$  at the time when a crack starts to grow. From the table, the values of  $\mathcal{E}_{\varphi_{max}}^I$  are judged to be almost constant. That is,  $\mathcal{E}_{\varphi_{max}}^I$  criterion expressed as  $\mathcal{E}_{\varphi_{max}}^I = (\mathcal{E}^I)_i$  is considered to be available for the experimental results. In Fig.14,  $(\sigma_{net})_i$  at the onset of crack growth obtained by the experiment is compared with the result by  $\mathcal{E}_{\varphi_{max}}^I$  criterion when  $(\mathcal{E}^I)_i [= (J_I)_i] = 0.042 J/mm^2$ . In the figure, the result by  $J_I + J_{II} = (J_I)_i$  criterion and the results by  $\sigma_{\theta_{max}}$  criterion and  $\mathcal{E}_{\varphi_{max}}^I$  criterion in case that the material is supposed to be an elastic one are also shown in the same way as in Fig.9. Moreover, yield stress  $\sigma_{ys}$  is shown for reference. From Fig.14, it is seen that the experimental result differs from the results by the criteria for elastic fracture, but agrees well with the result estimated from  $\mathcal{E}_{\varphi_{max}}^I$  criterion for elastic-plastic fracture over the entire range of  $\alpha$ . The result estimated from  $J_I + J_{II} = (J_I)_i$  criterion agrees with the experimental result tolerably but is a little larger than the experimental result.

Since the thickness of the specimen is thin, the fracture mode changes from the tearing one to the shearing one immediately after the onset of crack growth and, as shown in Fig.15, the direction,  $\varphi_0$ , observed on the surface of specimen does not show the real direction of crack growth. So, we regard the average of  $\varphi_0$  on the both surfaces of specimen as the direction of crack growth  $\varphi_i$ . In Fig.16, the results of the direction of crack growth experimentally obtained in this way are compared with the direction where  $\mathcal{E}_{\varphi}^I$  takes  $\mathcal{E}_{\varphi_{max}}^I$ . The experimental result agrees well in the figure with the direction,  $\varphi_i$ , where  $\mathcal{E}_{\varphi}^I = \mathcal{E}_{\varphi_{max}}^I$  and it is seen that the direction of crack growth can be also estimated by  $\mathcal{E}_{\varphi_{max}}^I$  criterion.

Considering the facts above in addition to the discussions in the previous chapters, it can be concluded now that  $\mathcal{E}_{\varphi_{max}}^I$  criterion is effective from completely elastic fracture to elastic-plastic fracture with large yielding region in a unified way. Here, it may be said from Figs.9 and 13 that, when  $\alpha$  is comparatively small,  $J_I + J_{II} = (J_I)_i$  and  $J_I + cJ_{II} = (J_I)_i$  criteria are also applicable. However, it should be noted that these criteria can not be used

Table 1  $\mathcal{E}_{\varphi_{max}}^I$  and  $(u)_i$  for each  $\alpha$

$\alpha$ (DEG.)	0	30	60	75
$\mathcal{E}_{\varphi_{max}}^I$ (J/mm <sup>2</sup> )	0.042	0.042	0.045	0.044
$(u)_i$ (mm)	0.36	0.37	0.46	0.62

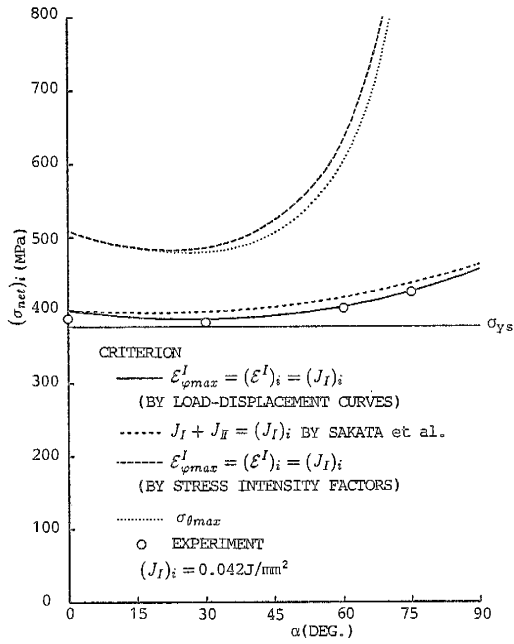


Fig.14 Relationship between  $(\sigma_{net})_i$  and  $\alpha$

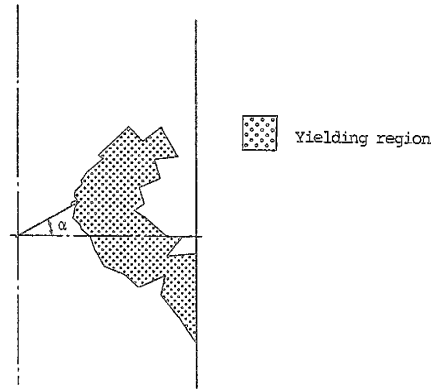


Fig.13 Yielding region of specimen ( $\alpha = 30^\circ$ )

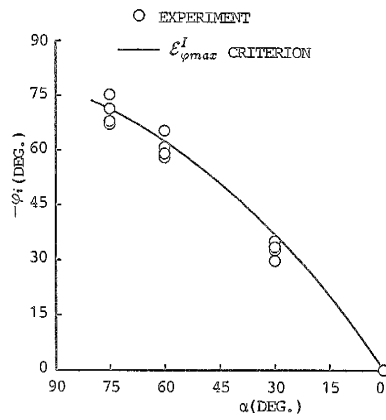


Fig.16 Comparison between crack growth direction by experiment and  $\mathcal{E}_{\varphi_{max}}^I$  criterion

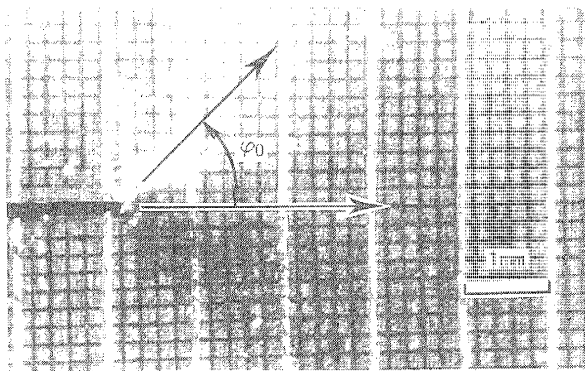


Fig.15 Crack growth direction ( $\alpha = 0^\circ$ )

to estimate elastic (quasi-elastic) fracture and can not estimate the direction of crack growth in addition to the fact that their physical meanings are not clear.

By the way, though Aluminum alloy 2024-T3 is used both in the present experiment and the experiment by Takamatsu et al., the experimental results (for instance, the loading point displacement at the onset of crack growth etc.) for each experiment are considerably different. The relative velocity of the crosshead in the experiment by Takamatsu et al. is  $1.0\text{mm}/\text{min}$  and different from the present one. But, as shown in Fig.12, it seems that the material constants almost do not depend on the relative velocity of crosshead. As for the material constants in the experiment by Takamatsu et al., Young's modulus  $E = 70.61\text{GPa}$ , Poisson's ratio  $\nu = 0.325$ , Yield stress  $\sigma_{ys} = 377.3\text{MPa}$  and  $C = 1039.5\text{MPa}$  and  $n = 0.31$  and  $e = 0.038$  in  $\bar{\sigma} = C(e + \bar{\epsilon}_p)^n$ . When they are compared with the material constants for the present experiment,  $E$ ,  $\nu$  and  $\sigma_{ys}$  are almost the same, but the strain hardening curve is considerably different. It seems that the difference of each experimental result depend on the difference of the hardening property in elastic-plastic region.

## 6 CONCLUSION

The applicability of the mixed-mode fracture criterion based on the CED in an arbitrary direction ( $\mathcal{E}_{\varphi_{max}}^I$  criterion) was studied. For elastic (quasi-elastic) fracture, the result estimated by  $\mathcal{E}_{\varphi_{max}}^I$  criterion was compared with the results by other criteria and experimental results. For elastic-plastic fracture,  $\mathcal{E}_{\varphi_{max}}^I$  criterion was applied to the fracture experiments of the thin specimens with an inclined crack under tensile loading. Through the discussions, it was shown that  $\mathcal{E}_{\varphi_{max}}^I$  criterion can be a criterion for a mixed mode crack effective from completely elastic fracture to elastic-plastic fracture with large yielding region in a unified way.

## REFERENCES

- Erdogan, F and Sih, G.C. (1963). On the Crack Extension in Plates Under Plane Loading and Transverse Shear, Transactions of the ASME, Ser.D, Vol.85, No.4, pp.519-527.
- Sih, G.C. (1973). SOME BASIC PROBLEMS IN FRACTURE MECHANICS AND NEW CONCEPTS, Engineering Fracture Mechanics, Vol.5, pp.365-377.
- e.g. Kageyama, K. and Okamura, H. (1982). Transactions of the JSME, Ser.A, Vol.48, No.430, pp.783-791.
- Takamatsu, T. and Ichikawa, M. (1987). Mixed Mode Fracture Criterion in Thin Sheets of 2024-T3 Al-alloy, Transactions of the JSME, Ser.A, Vol.53, No.486, pp.246-249.
- Sakata, M., Aoki, S., Kishimoto, K., Takizawa, M. and Chikugo, H. (1985). Mixed Mode Ductile Fracture of 2024-T351 Al-alloy, Transactions of the JSME, Ser.A, Vol.51, No.469, pp.2129-2136.
- Cotterell, B., Lee, E. and Mai, Y. (1982). Mixed Mode Plane Stress Ductile Fracture, International Journal of Fracture, Vol.20, pp.243-250.
- Watanabe, K. (1981). New Proposal of Crack Energy Density Concept as a Fundamental Fracture Mechanics Parameter, Bulletin of the JSME, Vol.24, No.198, pp.2059-2066.
- Watanabe, K. (1983). On the Crack Energy Density and Energy Release Rate for an Erasto-plastic Crack, Bulletin of the JSME, Vol.26, No.215, pp.747-754.
- Watanabe, K. and Shiomi, H. (1985). Extension of Crack Energy Density Concept to Arbitrary Direction and Energy Release Rate to Non-self-similar Crack Growth, Bulletin of the JSME, Vol.28, No.245, pp.1077-1084.
- Watanabe, K. and Utsunomiya, T. (1987). Separation of Each Deformation Mode

- Contribution from Total Crack Energy Density and Its Evaluation by Path-Independent Integral, Transactions of the JSME, Vol.53, No.491, pp.1285-1292.
- Watanabe,K., Utsunomiya,T. and Hirano,Y. (1989). CED (Crack Energy Density) in an Arbitrary Direction and Load-Displacement Curves, JSME International Journal, Ser. I, Vol.32, No.4, pp.527-534.
- Watanabe,K., Utsunomiya,T. (1989). A Fundamental Study on the Evaluation and Applicability as a Mixed-mode Fracture Criterion of Crack Energy Density in an Arbitrary Direction, Transactions of the JSME, Ser.A, Vol.55, No.516, pp.1832-1840.
- Watanabe,K., Utsunomiya,T., (1990). Applicability of CED (Crack Energy Density) to Mixed Mode Fracture Problem, International Journal of Pressure Vessel and Piping, Vol.44, pp.175-189.
- Shiomi,H. (1981). Master Thesis, University of Tokyo.
- Williams,J.G. and Ewing,P.D. (1972). Fracture under Complex Stress - The Angled Crack Problem, International Journal of Fracture Mechanics, Vol.8, No.4, pp.441-446.
- Kitagawa,T. and Yuuki,R. (1977). Analyses of Arbitrary Shaped Crack in a Finite Plate by Conformal Mapping, Transactions of the JSME, Ser.A, Vol.43, No.376, pp.4354-4362.
- Ichikawa,M. and Takamatsu,T. (1984). Fracture Mechanics Approach to Fracture Behavior of Center Cracked Sheet Specimens of 2024-t3 Aluminum Alloy under Mode II Loading, Transactions of the JSME, Ser.A, Vol.50, No.453, pp.959-965.